Supplementary material for "Evaluation of debris-flow building damage forecasts"

Katherine R. Barnhart[1], Christopher R. Miller[2], Francis K. Rengers[1], and Jason W. Kean[1]

1 U.S. Geological Survey, Geologic Hazards Science Center, Box 25046 DFC MS 966, Denver, CO 80225-0046, USA
2 Unaffiliated, Denver, CO, USA

Correspondence to: Katherine R. Barnhart (krbarnhart@usgs.gov)

Any use of trade, product, or firm names is for descriptive purposes only and does not imply endorsement by the U.S. Government.

Table S1. Building damage states, 2018 Montecito debris-flow event.

	Damage state classification	Domain			
CAL FIRE inspection damage state	D_s	Montecito	San Ysidro	Romero	Total†
Unimpacted *	0	1753	1380	986	4002
Affected	0	60	14	53	127
Minor damage	0	52	44	32	126
Major damage	1	57	37	21	114
Destroyed	1	54	94	14	162
Total number of impacted buildings		223	189	120	529
Total number of buildings		2199	1758	1226	5060

Notes: * Unimpacted building from Open Street Map.

†One hundred and seventeen unimpacted, two minor damage, and one major damage state buildings present in overlapping portions of the simulation domains.

CAL FIRE -- California Department of Forestry and Fire Protection

Table S2. Volume ranges for event magnitude forecast bias

Event magnitude forecast bias	Interpretation	Volume range (mean), 10^3 m^3			Number of simulations*		
		Montecito domain	San Ysidro domain	Romero domain	Montecito domain	San Ysidro domain	Romero domain
Very underforecast	Observed event size was larger than forecast	<186 (139)	<186 (137)	<117 (108)	160/268/140	160/268/56	44/68/36
Underforecast		186–372 (270)	186–372 (273)	117–234 (170)	180/304/192	180/304/92	176/304/204
Unbiased	Observed event size was correctly forecast	372–741 (538)	372–741 (532)	234–468 (341)	180/300/168	180/300/152	180/296/204
Overforecast		741–1480 (1069)	741–1480 (1082)	468–933 (669)	180/300/184	180/300/164	180/304/208
Very overforecast	Observed event size was smaller than forecast	>1480 (2889)	>1480 (2898)	>933 (2435)	320/528/400	320/528/404	440/728/556

Note: *Number of simulations indicated as R/F/D where R, F, and D are the number of simulations from RAMMS, FLO-2D, and D-Claw, respectively (Christen et al., 2010; George and Iverson, 2014; Iverson and George, 2014; O'Brien et al., 1993; O'Brien, 2020.

Table S3. Distribution of number of stories in buildings damaged by the Montecito event.

Number of stories	Count	Percent
1	165	83.3%
2	33	16.7%

Table S4. Distribution of building ages in buildings damaged by the Montecito event.

Building age	Count	Percent
Before 1941	29	18.0%
1941-1975	84	52.2%
After 1975	48	29.8%

Table S5. Logistic regression fit for prediction of simplified damage state (D_s).

	Dependent variable:
	D_s
ln(h), β_1	2.521^{***} (2.175, 2.867)
Constant, β_0	1.927^{***} (1.584, 2.269)
Number of observations	4,531
Log Likelihood	-202.693
Akaike Information Criterion	409.386

Note:

Significance levels denoted by asterixis: * indicates $p<0.1$, ** indicates $p<0.05$, and *** indicates $p<0.01$, where p is the probability the coefficient is not zero. Values given in parenthesis denote the 90% confidence interval for the coefficient.

Table S6. Forecast performance metrics for probabilistic forecasts for simplified damage state (D_s) by model.

Model	Independent variable	Volume class*	True positive	False positive	True negative	False negative	False Alarm Ratio	Hit rate	Bias	Threat Score
RAMMS	h	1	0.01	0.01	0.93	0.05	0.40	0.21	0.35	0.18
RAMMS	hv^2	1	0.00	0.00	0.94	0.06	0.58	0.03	0.07	0.03
RAMMS	h	2	0.03	0.05	0.89	0.03	0.64	0.46	1.27	0.25
RAMMS	hv^2	2	0.01	0.01	0.93	0.05	0.57	0.12	0.29	0.11
RAMMS	h	3	0.04	0.13	0.81	0.02	0.76	0.67	2.84	0.21
RAMMS	hv^2	3	0.02	0.03	0.91	0.05	0.67	0.25	0.76	0.17
RAMMS	h	4	0.05	0.24	0.70	0.01	0.84	0.77	4.73	0.15
RAMMS	hv^2	4	0.02	0.07	0.87	0.04	0.76	0.36	1.53	0.17
RAMMS	h	5	0.05	0.35	0.59	0.01	0.88	0.81	6.59	0.12
RAMMS	hv^2	5	0.03	0.20	0.74	0.03	0.86	0.53	3.80	0.12
FLO-2D	h	1	0.01	0.01	0.93	0.05	0.29	0.22	0.32	0.21
FLO-2D	hv^2	1	0.00	0.00	0.94	0.06	0.40	0.01	0.02	0.01
FLO-2D	h	2	0.04	0.05	0.89	0.03	0.56	0.58	1.32	0.33
FLO-2D	hv^2	2	0.01	0.00	0.94	0.06	0.38	0.09	0.14	0.09
FLO-2D	h	3	0.05	0.16	0.78	0.01	0.77	0.78	3.39	0.22
FLO-2D	hv^2	3	0.01	0.02	0.92	0.05	0.61	0.16	0.42	0.13
FLO-2D	h	4	0.06	0.34	0.60	0.01	0.86	0.92	6.47	0.14
FLO-2D	hv^2	4	0.02	0.05	0.89	0.04	0.71	0.30	1.05	0.17
FLO-2D	h	5	0.06	0.58	0.36	0.00	0.91	0.97	10.50	0.09
FLO-2D	hv^2	5	0.04	0.26	0.68	0.02	0.87	0.65	4.88	0.12
D-Claw	h	1	0.00	0.00	0.94	0.06	1.00	0.00	0.00	0.00
D-Claw	hv^2	1	0.00	0.00	0.94	0.06	0.50	0.00	0.01	0.00
D-Claw	h	2	0.03	0.03	0.91	0.03	0.50	0.43	0.86	0.30
D-Claw	hv^2	2	0.01	0.01	0.93	0.05	0.53	0.18	0.39	0.15
D-Claw	h	3	0.04	0.10	0.84	0.02	0.71	0.70	2.38	0.26
D-Claw	hv^2	3	0.03	0.06	0.88	0.03	0.66	0.48	1.43	0.25
D-Claw	h	4	0.05	0.27	0.67	0.01	0.83	0.88	5.30	0.16
D-Claw	hv^2	4	0.05	0.20	0.74	0.02	0.81	0.74	3.97	0.17
D-Claw	h	5	0.06	0.52	0.41	0.00	0.90	0.96	9.58	0.10
D-Claw	hv^2	5	0.05	0.48	0.46	0.01	0.90	0.89	8.80	0.10

Note: *Volume class values of 1, 2, 3, 4, and 5 refer to very underforecast, underforecast, unbiased, overforecast, and very overforecast event magnitude forecast bias categories, respectively.

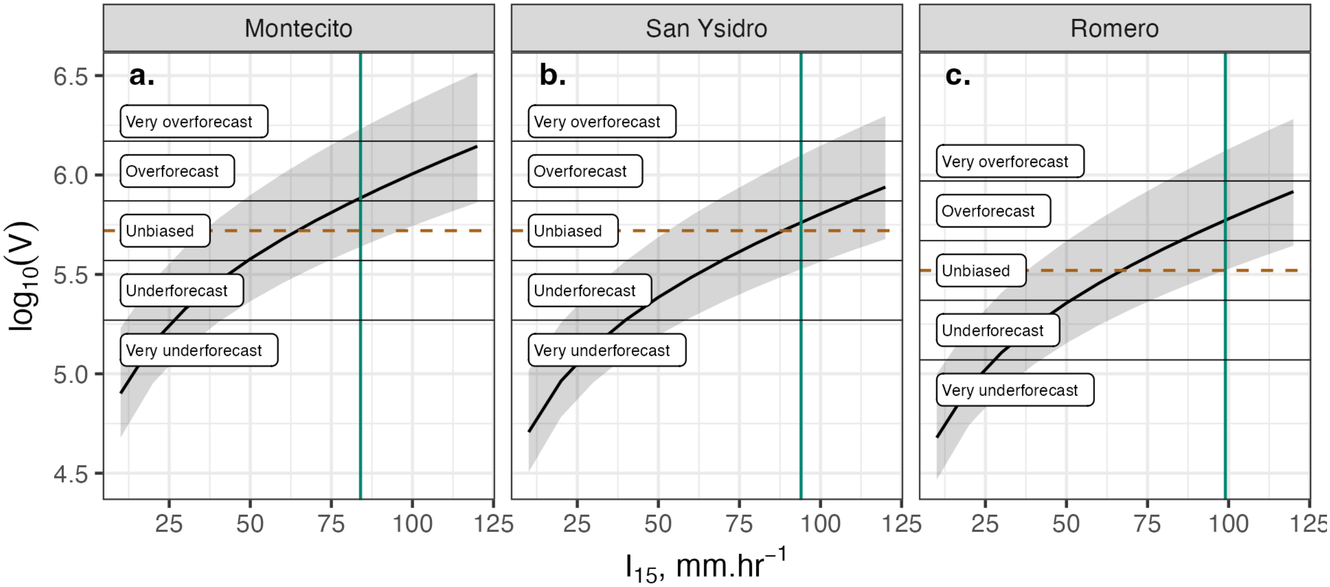

Figure S1. Relation between 15-minute rainfall intensity, I_{15}, and simulated event size, log(V), depicted as the black curved line, with 95% confidence intervals depicted as the grey shaded region. The simulated event size comes from combining the sediment volume produced by the U.S. Geological Survey hazard assessment for the Thomas Fire (U.S. Geological Survey, 2018) generated using the Gartner et al. (2014) empirical model and the volume of water that would fall on the considered basins in 15 minutes. The estimated rainfall for each domain is depicted as the vertical green line and the estimated event size as the horizontal brown dashed line. Thin black horizontal lines depict the boundaries between the five event magnitude bias volume classes.

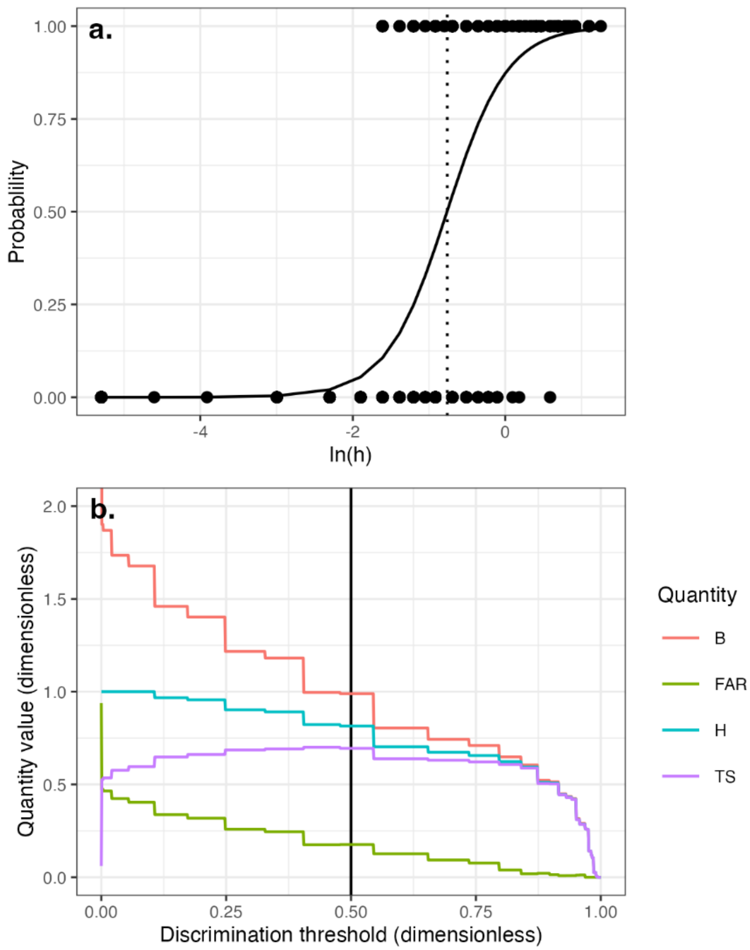

Figure S2. Probability of the simplified damage state (D_s) being equal to one (damage occurring) as a function of natural logarithm of debris-flow depth (ln(h)) based on the logistic regression model (a) and the variation in bias (B), false alarm ratio (FAR), the hit rate (H), and the threat score (TS) as a function of the discrimination threshold (b). Black dots in (a) depict data used to fit the logistic regression model (curved black line). The critical value for the threshold probability was selected as 0.5 because that value maximizes the TS and puts B near unity (b) and corresponds to a value of ln(h) of -0.76 or a value for h of 0.47 m (dashed vertical line in (a)).

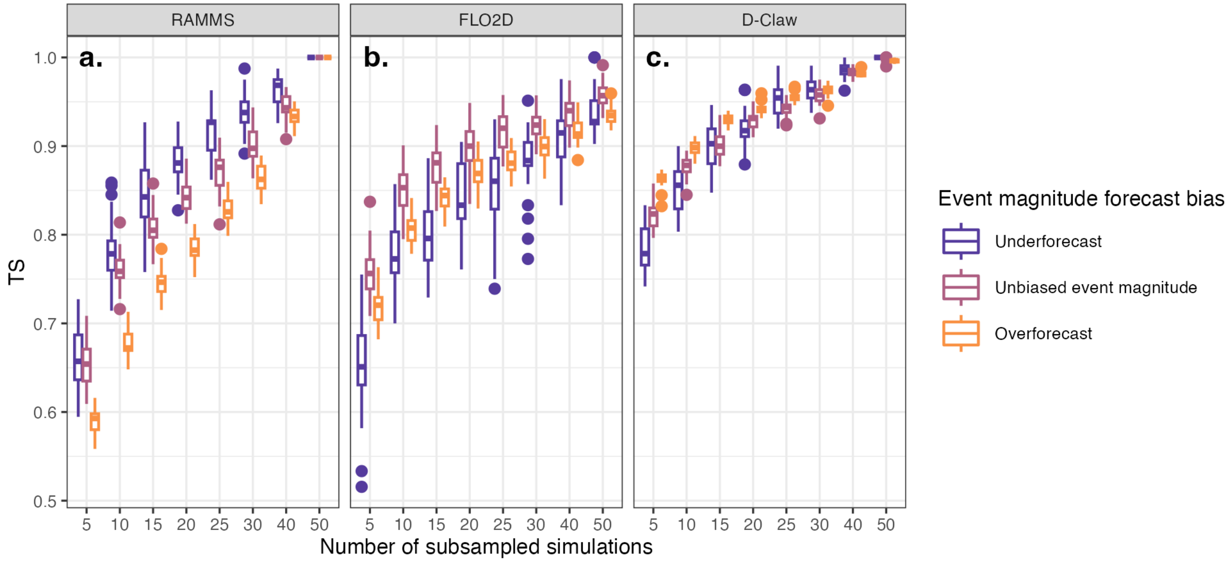

Figure S3. Consistency between forecasts generated by the full set of simulations and subsampled sets of simulations from the bootstrapping analysis as measured by the threat score, TS. Boxplots show the distribution of TS as a function of the number of subsampled simulations for three models and three event magnitude forecast bias categories. Boxplot depicts 25th, 50th, and 75th percentiles as horizontal lines; whiskers extend vertically to the observation no farther than 1.5x the interquartile range; and dots depict any outlying points.

References

Christen, M., Kowalski, J., and Bartelt, P.: RAMMS: Numerical simulation of dense snow avalanches in three-dimensional terrain, Cold Reg. Sci. Technol., 63, 1–14, https://doi.org/10.1016/j.coldregions.2010.04.005, 2010.

Gartner, J. E., Cannon, S. H., and Santi, P. M.: Empirical models for predicting volumes of sediment deposited by debris flows and sediment-laden floods in the transverse ranges of southern California, Eng. Geol., 176, 45–56, https://doi.org/10.1016/j.enggeo.2014.04.008, 2014.

George, D. L. and Iverson, R. M.: A depth-averaged debris-flow model that includes the effects of evolving dilatancy. II. Numerical predictions and experimental tests, Proc. R. Soc. Math. Phys. Eng. Sci., 470, 20130820, https://doi.org/10.1098/rspa.2013.0820, 2014.

Iverson, R. M. and George, D. L.: A depth-averaged debris-flow model that includes the effects of evolving dilatancy. I. Physical basis, Proc. R. Soc. Math. Phys. Eng. Sci., 470, 20130819, https://doi.org/10.1098/rspa.2013.0819, 2014.

O'Brien, J. S.: FLO-2D reference manual, Tech. Rep., https://documentation.flo-2d.com/, 2020.

O'Brien, J. S., Julien, P. Y., and Fullerton, W. T.: Two-dimensional water flood and mudflow simulation, J. Hydraul. Eng., 119, 244–261, https://doi.org/10.1061/(ASCE)0733-9429(1993)119:2(244), 1993.

OpenStreetMap contributors: Planet dump retrieved from https://planet.osm.org, 2021.

U.S. Geological Survey: Emergency assessment of post-fire debris-flow hazards, 2017 Thomas Fire, retrieved from https://landslides.usgs.gov/static/landslides-realtime/fires/20171204_thomas/PostFireDebrisFlowEstimates.zip, 2018.